Biomaterials Science

Accepted Manuscript

This article can be cited before page numbers have been issued, to do this please use: M. Wekwejt, S. Chen, B. Kaczmarek, M. Nadolska, K. P. ukowicz, A. Paubicka, A. Michno, A. M. Osyczka, M. Michalek and A. Zieliski, *Biomater. Sci.*, 2021, DOI: 10.1039/D1BM00079A.

ROYAL SOCIETY OF CHEMISTRY

rsc.li/biomaterials-science

View Article Online
DOI: 10.1039/D1BM00079A

ARTICLE

Nanosilver-loaded PMMA bone cement doped with different bioactive glasses – evaluation of cytocompatibility, antibacterial activity, and mechanical properties

Received 00th January 20xx,
Accepted 00th January 20xx

DOI: 10.1039/x0xx00000x

M. Wekwejt,*[a] S. Chen, [b] B. Kaczmarek, [c] M. Nadolska, [d] K. Łukowicz, [e] A. Pałubicka, [f] A. Michno, [g] A.M. Osyczka, [e] M. Michálek, [b] and A. Zieliński [a]

Nanosilver-loaded PMMA bone cement (BC-AgNp) is a novel cement developed as a replacement for conventional cements. Despite favorable properties and antibacterial activity, BC-AgNp still lacks biodegradability and bioactivity. Hence, we investigated the doping with bioactive glasses (BGs) to create a new bioactive BC characterized by time-varying porosity and gradual release of AgNp. The BC Cemex was used as the base material and modified simultaneously with the AgNp and BGs: melted 45S5 and 13-93B3 glasses with various particles size and sol-gel derived SiO2/CaO microparticles. The effect of BGs addition was examined by microscopic analysis, an assessment of setting parameters, wettability, FTIR and UV-VIS spectroscopy, mechanical testing, hemo- and cytocompatibility and antibacterial efficiency studies. The results show that it is possible to incorporate various BGs into BC-AgNp that lead to different properties depending on the type and size of BGs. The smaller particles of melted BGs showed higher porosity and better antibacterial properties with the moderate deterioration of mechanical properties. The sol-gel derived BGs, however, displayed a tendency for agglomeration and random distribution in BC-AgNp. The BGs with greater solubility more efficiently improves the antibacterial properties of BC-AgNp. Besides, the unreacted MMA monomer release could negatively influence the cellular response. Despite that, the cements doped with different BGs are suitable for medical applications.

1 Introduction

Human bones exhibit unusual biological and mechanical properties. They are able to withstand large forces, bear heavy loads, flex to some limit without fracture, and most importantly they have a natural ability to self-healing[1]. Severe bone injuries due to complicated fractures or critical bone defects followed by the resection of tumours require biocompatible artificial replacement to support the patient's life quality[2]. Bone cements form an attractive biomaterial group as they are widely used for defect filling, fracture stabilization, and implant fixation especially cements based on poly(methyl methacrylate) (PMMA)[3-5]. Acrylic bone cements (BCs) are characterized by beneficial functional properties, such as easy processability, fast polymerization, favorable mechanical properties, injectable capability, and high biostability in the human body[5-6]. Moreover, the increasing interest in BCs is attributed to their use as a drug delivery system (antibiotic treatment or local chemotherapy) or antibacterial coatings of implants[7-9]. However, most drugs added to BCs are permanently locked in their low-porous and non-biodegradable structure and only a small dose is released from the surface layers, mainly within the first few days after implantation[10]. Furthermore, BC is a bioinert material without osseointegrative properties, which may result in limited integration with host bone tissue and future ineffective biofunctionality[11].

Numerous studies were aimed at the improvement of BCs biological or mechanical properties, mainly by adding modifiers as reinforcement components[12-14], biodegradable fillers[15,16], bioactive additives[17,18], and antibacterial agents[19-21]. Research is also underway to increase the antibacterial effectiveness of BCs by selecting the appropriate antibiotic or improving its release[22,23]. However, besides antibiotics, there may be other antibacterial additives for BCs such as nanometals[24-26]. Particularly noteworthy is nanosilver (AgNp), which is characterized by high bactericidal ability and a broad spectrum of activity resulting in the elimination of the problem of bacterial resistance[27,28]. As we have previously reported, the addition of low content of nanometals (1.5 wt.%) does not influence the physical and mechanical properties of BC and may provide antibacterial protection, but it may negatively affect

[a] Biomaterials Division, Faculty of Mechanical Engineering and Ship Technology, Gdańsk University of Technology, Gdańsk, Poland.
[b] Centre for Functional and Surface Functionalized Glass, TnU AD, Trenčín, Slovakia.
[c] Department of Chemistry of Biomaterials and Cosmetics, Faculty of Chemistry, Nicolaus Copernicus University in Toruń, Toruń, Poland.
[d] Faculty of Applied Physics and Mathematics, Gdańsk University of Technology, Gdańsk, Poland.
[e] Department of Biology and Cell Imaging, Institute of Zoology and Biomedical Research, Faculty of Biology, Jagiellonian University, Kraków, Poland.
[f] Department of Laboratory Diagnostics and Microbiology with Blood Bank, Specialist Hospital in Kościerzyna, Kościerzyna, Poland.
[g] Chair of Clinical Biochemistry, Department of Laboratory Medicine, Medical University of Gdańsk, Gdańsk, Poland.
E-mail: marcin.wekwejt@pg.edu.pl
† Electronic Supplementary Information (ESI) available: [details of any supplementary information available should be included here]. See DOI: 10.1039/x0xx00000x

biocompatibility, depending on the type and properties of nanometals[24,25]. Furthermore, we have evaluated different biodegradable additives (cellulose, chitosan, magnesium, polydioxanone, and tri-calcium phosphate) to obtain partially-degradable BC characterized by additional bioactivity. We have shown that these additives successfully increase the porosity of BCs and accelerate the active substance release, however, they may deteriorate mechanical properties and decrease cytocompatibility. Based on the obtained results, we have concluded that 5 wt.% is the optimal content of additive in BCs and hypothesized that reducing the particle size of the additives could solve above mentioned issues[26].

Continuing our research on developing bioactive BC, we have decided to modify it simultaneously with AgNp and bioactive glasses (BGs). We have chosen two of the most common BGs used in the medical aspect, namely silicate and borate. These glasses are biodegradable materials and have also osteoconductive properties that make them potentially useful as modifiers. As the BGs particles dissolve, the released products may stimulate new bone growth or a hydroxycarbonate apatite layer formation on the material surface the cell adhesion[29-31]. The different composition of the selected BGs affects some other properties, such as aqueous solubility and osteoinductivity, hence, they may differently influence the BC properties after their incorporation. We assume that these additives may improve the antibacterial effectiveness of AgNp-doped BC without affecting its other features. Recently, there have been some reports regarding the development of bioactive composites based on PMMA and BGs as drug delivery systems[32,33], the coatings of implants[34,35] or bone substitutes[36-38]. Moreover, there have been some studies suggesting that BGs may be used as a BC modifier to promote bioactivity[39,40], to increase mechanical strength[41], or to improve antibiotic release[42]. However, best to our knowledge, there are no literature reports presenting studies of doping BGs into AgNp-loaded BCs and evaluating the properties of such cement-based composites. Hence, in this study, we have aimed to develop novel cement simultaneously modified with AgNp and different BGs: two melted glasses 45S5; 13-93B3 with two particles size, namely ≥ 40 μm or between 40 – 80 μm, and sol-gel obtained SiO_2/CaO glass with particles size ~ 300 nm. The chemical composition of such composite BCs and their structure, physical, mechanical and biological properties have been characterized. Our main goal has been to develop a new formula of modified BC with advantageous properties with respect to classical BCs, in particular characterized by partially-degradable structure and a significant antibacterial effectiveness against antibiotic-resistant bacteria.

2 Materials and Methods

2.1 Cement preparation

The PMMA bone cement Cemex (Tecres Company, Italy) was used as the base material modified with the BGs (5 wt.%) and the AgNp (1.5 wt.%). The contents of modifiers were selected based on our previous research[24-26]. The process of obtaining BGs was described below. AgNp (50 nm, average particle size, 99.9% purity) was purchased from MkNano Company (MkNano, Canada). The BCs composition is presented in Table 1 and its liquid-to-powder ratio was 0.33[43].

Table 1. Chemical composition of bone cements and additives' specifications.

Nanosilver characteristics	Bioactive glass name and grain size		Powder composition	Liquid Composition
AgNp powder (MkNano), particle size: ~50 nm, spherical shape, 99.9% purity	BG-0.4 BG-0.8 BGII-0.4 BGII-0.8	45S5; ≥ 40 μm 45S5; 40 – 80 μm 13-93B3; ≥ 40 μm 13-93B3; 40 – 80 μm	polymethyl methacrylate (84.30 %) barium sulfate (13.00 %) benzoyl peroxide (2.70 %)	methyl methacrylate (99.1 %) N,N-dimethyl-p-toluidine (0.9 %) hydroquinone (75 ppm)
	BG-MP	SiO2/CaO (70/30 mol %); ~ 300 nm		

All BC specimens with/without modifications were prepared as described earlier[24-26]. For the modified BCs, the BGs and/or AgNp powders were added into cement powder and manually mixed for about 1 min or until the visual homogenous distribution of powders was observed. The BC specimens were prepared by manually mixing the liquid component with the powder in a bowl until the development of a macroscopically homogenous paste. The paste was then placed into molds and allowed to cure for 1 h under ambient conditions.

2.2 Bioactive glass synthesis

The following types of BGs were used in the research: (i) a melted glass with a composition of 45S5 Bioglass® (wt%: 45 SiO_2, 24.5 CaO, 24.5 Na_2O, and 6 P_2O_5) with particles size ≥ 40 μm or between 40 – 80 μm, (ii) a melted glass with the composition of 13-93B3 (wt%: 56.6 B_2O_3, 18.5 CaO, 11.1 K2O, 5.5 Na_2O, 4.6 MgO, 3.7 P_2O_5), particles size ≥ 40 μm or between 40 – 80 μm and (iii) sol-gel derived SiO_2/CaO (70/30 mol%) with spherical particles with a diameter of ~ 300 nm. The following reagent grade reactants were used to fabricate the mentioned glassess, BG: SiO_2, $CaCO_3$, Na_2CO_3 (CentralChem, Slovakia) and $Na_5P_3O_{10}$ (Merck, Germany); BGII: H_3BO_3, $CaCO_3$, K_2CO_3, Na_2CO_3, MgO (CentralChem, Slovakia) and $Na_5P_3O_{10}$ (Merck, Germany) and BG-MP $(C_2H_5O)_4Si$ (AlfaAesar, USA), $Ca(NO_3)_2{\cdot}4H_2O$ (CentralChem, Slovakia) and NH_3 (Merck, Germany). The mixed and homogenized powders for melted BGs were heated in a high-temperature furnace (Classic 0718E, Czech Republic) to 1350 °C (BG) or 1000 °C (BGII) for 4h inside a platinum crucible, next the melts were cast into stainless steel plates, annealed (~520 °C/30 min) and cooled at ambient temperature in a muffle furnace (LAC, Czech Republic). The produced bulk glass was crushed to glass chips, then milled in a zirconia ball milling machine (Fritsch, Germany) and sieved in a laboratory sieve shaker (Retsch, Germany) to obtain powders with the required size range. The BG-MP was prepared by the Stöber method modified by Zheng et al.[44]. Briefly, the first solution composed of 4.5 mL of ammonium hydroxide solution (28-30% NH_3; Merck, Germany), 8.12 mL of ethanol (99.8%; CentralChem, Slovakia), and 12.38 mL of deionized H_2O was continuously stirred and then mixed with the second solution prepared by dissolving 2.25 mL of tetraethyl phosphate (TEOS, 98%; AlfaAesar, USA) in 25 mL of ethanol. After 30 min, 1.45 g of calcium nitrate ($Ca(NO_3)_2$, 99%; CentralChem, Slovakia) was

added and the mixture was allowed to react for 1.5 h. The resulting whitish suspensions were centrifuged at 6000 rpm for ~15 min to obtain deposits (Eba 20, Hettich, Germany). The deposits were washed twice using deionized water and once using ethanol and dried overnight at 40°C. Finally, the collected deposits were calcinated at 700 °C for 3h. The morphology of the particles with the chemical composition was analyzed by scanning electron microscope (SEM; JEOL 7600, Japan) equipped with EDX detector (OXFORD instruments, X-Max, UK). The non-crystalline appearance was confirmed by X-ray diffraction (analytical Empyrean, 45 kV accelerating voltage, CuKα radiation with λ = 1.5405 Å, measured in the 2θ range 10°–80°).

2.3 Characterization

2.3.1 Setting measurements. The curing time of the BCs was performed using the Vicat needle apparatus (ZI-1004, Zeal International, India) with a tip diameter of 1 mm and 400 g load. The curing time was considered as the length of time starting from mixing the cement components to the moment that the specimens were solidified - the indentation mark was not visible on the surface. The polymerization temperature was monitored continuously using a thermocouple 13-R (Czah, Poland). The probe was placed into a mould filled with BC dough and the temperature changes were recorded at 10 s intervals to determine the maximum polymerization temperature (T_{max}).

2.3.2 Microscopic analyses. The surface microstructure of the BCs, before and after soaking in the phosphate-buffered saline (PBS) solution, was examined using a high-resolution scanning electron microscope (SEM; JSM-7800F, Jeol, Japan) and ultra-high accuracy digital optical microscope OM (VHX-7000 S770E, Keyence, Japan). All specimens were sputtered with a thin (5 nm) chromium layer for electron reflection before the SEM examination. BCs porosity was assessed from the changes in surface images by microscopic observations. Moreover, the Cavalieri-Hacquert principle was adopted assuming that the internal porosity of the matrix should be similar to that of the surface[45].

2.3.3 Fourier transform infrared spectroscopy – attenuated total reflectance (FTIR-ATR). The functional groups and chemical bonds of specimens were analyzed by FTIR-ATR in the range 4000-600 cm^{-1} with 64 scans and resolution 4 cm^{-1}. The spectrometer equipped with diamond crystal (Nicolet iS110, Thermo Fisher Scientific Inc., USA) was used for all types of BCs and the measurements were made on their surface as well as on their cross-sections. The spectra were acquired in the absorbance mode, normalized and smoothed.

2.3.4 Surface wettability. The surface wettability was determined by water contact angle measurements with an optical tensiometer (Attention Theta Life, Biolin Scientific, Finland) based on the falling drop method. The volume of the drop was approximately 1 µL; each measurement was carried out five times, immediately after the drop fall.

2.4 PBS exposure and UV-VIS analysis

The BC specimens (n=3) in disk form (20x2 mm) were immersed in 5 mL of PBS solution (Merck, Germany) and stored at 37°C for 30 days. After the immersion, the specimens were removed from the solution, rinsed and dried overnight, then weighed. Their relative changes in weight after PBS exposure were calculated. These specimens were also used for mechanical tests and SEM analyses. Furthermore, the effect of PBS exposure, in particular on the release of MMA monomer and AgNp from the BC matrix, was evaluated by the UV-VIS spectrometer (Evolution 220, Thermo Fisher Scientific, USA). The more detailed measurement protocol was presented in our previous report[26]. Briefly, the absorption spectra of the immersion solutions were measured after 1, 7, and 30 days, in the range from 200 to 500 nm and PBS was used as a blank. The characteristic peak for MMA is at ~220 nm, while AgNp peaks are at ~270 nm[46]. Additionally, the absorption spectrum of the AgNp/water suspension (0.01 g/L) was applied as a reference (SFig.1).

2.5 Mechanical properties

The mechanical properties of the BCs in the disk form before and after PBS exposure were determined by the microindentation technique with NanoTest™ Vantage equipment (Micro Materials, UK) already applied for BCs[47]. The experiments were performed using a three-sided diamond, a pyramidal indenter (Berkovich indenter). The following parameters were set up: 0.05 mm of the indentation depth, 20 s of the loading time, 15s of the unloading time and 5 s of the holding time under maximum force. The load-displacement curves were determined for each sample (n=10) and the hardness (H) and reduced Young's modulus (Er) were calculated by the Oliver and Pharr method[48] using integrated software. On the other hand, the creep at the viscoelastic/plastic contact of indenter-material, subsurface hydrostatic pressure, and pile-up phenomenon during the test, affected each test and made large standard deviations[49]. Moreover, because of the small surface area contact of Berkovich indenter (~55 μm^2), the scale effect occurred[47-49].

2.6 Hemo- and cytocompatibility

All the BC specimens were sterilized with 75% ethanol followed by 30 min exposure to UV light. The experiments were performed triplicate using specimens in a disk form (10x2 mm for hemocompatibility and 20x2 mm for cytocompatibility). The BCs biocompatibility was evaluated based on the procedures previously used and described[25].

2.6.1 Cells collection and preparation. Red blood cells (RBCs) and platelets (PLTs) were obtained from erythrocytes` and blood platelets` contaminated buffy coats delivered by the Regional Blood Centre in Gdańsk and provided as by-products of whole blood fractionations (Regional Blood Blank institutional permission: M-073/17/JJ/11). Whole blood was collected from healthy volunteers following the Declaration of Helsinki under an approved Regional Bank review board protocol in standard acid citrate dextrose solutions. RBCs and PLTs were fractionated according to the standards of Blood Banks[50]. The number of erythrocytes and platelets was

estimated with a hemocytometer Superior CE (Marienfeld, Lauda-Königshofen, Germany). The human periodontal ligament cells (PDLCs) were obtained from the molar tooth of 31–43 years old donors, both genders, under permission of the Polish Research Ethics Board (approval no. 1072.6120.253.2017). All experiments were performed in accordance with the Guidelines of "Directive 2004/23/EU of the European Parliament and of the Council " and were approved by the local Bioethics Committee at "the Jagiellonian University in Kraków". Informed consents were obtained from human participants of this study. The cells were isolated according to a Bakkar protocol[51], expanded and cultured in a culture medium composed of alpha-MEM supplemented with 15% fetal bovine serum (FBS), 0.1 mM 1-ascorbic acid phosphate and 1% antibiotics (10.000 U/mL of Penicillin-Streptomycin). When the cells reached a confluent monolayer, they were lifted from culture flasks using 0.25% Trypsin-EDTA.

2.6.2 Hemolysis assay and viability of erythrocytes. RBCs (3 × 10^9 cells/mL) were placed in 2 mL tubes containing BC specimens and incubated at 37 °C for up to 24 h. Then, samples were centrifuged at 100x g at room temperature for 3 min to obtain the supernatants for assessment of hemolysis at 540 nm wavelength by Ultrospect 3000pro spectrophotometer (Amersham-Pharmacia-Biotech, Cambridge, UK). RBCs treated with 0.2% Triton were set as a positive control - 100% of hemolysis rate. For LDH assay, collected supernatants were homogenized and solubilized in 0.2% v/v Triton X-100. The activity of LDH was assayed by spectrophotometric methods at 340 nm[52]**.** The high hemolysis rate and high concentration of extracellular LDH indicate damage to RBCs integrity. According to the literature, if the hemolysis rate is lower than the value of 5% and concentrations of LDH are below 15 µmol/min/1012 – RBC, materials are accepted as a normal request of clinical application[53]**.**

2.6.3 Platelet viability and aggregation. PLTs suspended in Tyrode's buffer (pH 7.4; 3 × 10^8/mL) were placed in 2 mL tubes containing BC specimens preincubated at 37 °C for 2 h. For the analyses of PLT viability, MTT assay (thiazolyl blue tetra-zolium bromide; Sigma Aldrich, Steinheim, Germany) that reflects cells mitochondrial activity was used. After 4 h of incubation at 37 °C in the dark, a dimethyl sulfide/sodium dodecyl sulfate (20%/3%, pH 4.8; Sigma Aldrich, Steinheim, Germany) was added to dissolve the reduced formazan product and the absorbance at 570 nm was read in a microplate VICTOR 1420 Multilabel Counter (PerkinElmer, Kraków, Poland). The results were compared to negative PLT control (incubated without BC), assumed as 100% of platelet mitochondrial metabolism and viability. The positive control was PLT solubilized by the addition of Triton X-100 at a final concentration of 0.2% by volume. For aggregation assay, PLT samples were transferred to fresh cuvettes, preincubated for 5 min at 37 °C and then activated by the addition of thrombin (0.1 U/mL). Aggregation (i.e., 0.05 IU) was conducted for 10 min in the aggregometer APACT (Labor, Hamburg, Germany).

2.6.4 Periodontal ligament cell viability. Human PDLCs are among the well-defined cell populations that display high osteogenic potential and can be relatively easily obtained from extracted teeth[54]. PDLCs at the density of 2.5 x 10^4 were suspended in 1 mL of culture medium and seeded on the surface of BC specimens in 24-well culture plates. The plates were incubated at 37 °C in an atmosphere containing 5% CO2. The medium was replaced with a fresh one every 48 h. Cell viability was evaluated at day 7 culture using the CellTiter 96 Aqueous One Solution Cell Proliferation Assay (MTS, Promega, Poland). The development of the colored product by live cells was assessed colorimetrically using the plate reader (SpectraMax iD3, Molecular Devices, San Jose), taking absorbance at 490 nm. The results were expressed as a percentage of live cells on the studied specimens compared to the neat BC (100%).

2.6.5 PDLCs morphology. PDLCs were cultured as described above. After 5 days of culture, their morphology in the close proximity to the tested BCs was observed with contrast-phase inverse microscope Axiovert 40 CFL (Zeiss, Oberkochen, Germany). For control, the cells were also seeded into standard culture plates (TCP) without any specimens.

2.7 Antibacterial properties

All BC specimens before antibacterial studies were sterilized with 75% ethanol followed by 30 min exposure to UV light. The experiments were performed using three specimens for each type of BC in disk form (10x2 mm for turbidity tests and 20x2 mm for bactericidal effectiveness tests).

2.7.1 Bacterial growth inhibition. The inhibition of bacterial growth was evaluated by measuring the turbidity of cultured bacteria broth incubated with BC specimens. The tests were carried out according to the McFarland standards[55], assuming the existence of direct relation between turbidity of cultured bacteria broth and the number of bacteria. Briefly, when the optical density of bacterial suspension is 1.0 McFarland index (iMS), the number of bacteria is 3 x 10^8 CFU/mL. The tests were performed using three different strains of bacteria: *Staphylococcus aureus* ATCC 29213, *Staphylococcus aureus* hospital strain, and *Escherichia coli* ATCC 25922, and their initial concentration set at 1.5 x 10^8 CFU/mL (0.5 iMS). The hospital strains originated from bone infections (obtained from the Specialist Hospital in Kościerzyna) were characterized by high antibiotic resistance. The bacteria were suspended in Trypticase Soy Broth (2.0 mL; Merck, Darmstadt, Germany), incubated with BC specimens at 36 °C. After each hour the optical density measurements were carried out using the DensiChEK Plus (BioMerieux, Montreal, QC, Canada). The maximum measuring range of this device was 4 iMS.

2.7.2 Bactericidal effectiveness test. The bactericidal effectiveness tests were performed using *S. aureus* hospital strain characterized by methicillin resistance (obtained from the Specialist Hospital in Kościerzyna) for selected BCs: unmodified (BC), antibiotic-loaded (BC-A) and two modified BCs with BGs and AgNp: BC-BG-0.4-AgNp and BC-BGII-0.4-AgNp. The prepared bacterial suspension (0.5 McFarland index, PBS solution) was applied to the tested BC surface placed on Mueller-Hinton agar plates and incubated for 48 h at 36 °C.

Then, specimens were transferred to a sterile saline solution and subjected to sonication for 1 min. During the sonication process, 10 µL of bacterial suspension was collected, seeded, and incubated on standard BD Columbia agar with 5% sheep blood at 36 °C. The obtained results after 24 h of bacterial culture were presented in the images, allowing to specify the colony-forming unit (CFU) value.

2.8 Statistics

Statistical analysis of the data was performed using commercial software (SigmaPlot 14.0, Systat Software, San Jose, CA, USA). The Shapiro–Wilk test was used to assess the normal distribution of the data. All the results were calculated as means ± standard deviations (SD) and statistically analyzed using one-way analysis of variance (one-way ANOVA). Multiple comparisons versus the control group between means were performed using the Bonferroni t-test with the statistical significance set at $p < 0.05$.

3 Results

3.1 The morphology of BC and modifiers

The morphologies of prepared BGs and as-delivered AgNp are shown in Fig. 1. The AgNp are characterized by a spherical shape and a size in the range of 30-80 nm (average ~50 nm). The obtained particles of BGs differ in shape, composition, and size. BGs particles obtained by melting and grinding technique are characterized by a random shape and size for BG/BGII-0.4 in the range 10-64 µm (average ~34 µm) and BG/BGII-0.8 in the range 45-100 µm (average ~67 µm). The BGs particles obtained by the sol-gel technique possess a regular spherical shape and their size is in the range 250-420 nm (~340 nm). Moreover, the form of the particles distribution in the BC matrix is also different (Fig. 1 (b)). BG-MP was distributed mostly on the surface creating specific agglomerates (with a diameter between 200-400 µm), while the other BGs particles were randomly and permanently located (hammered) in the matrix.

Fig. 1. SEM images of modifiers: I) AgNp, II) BG-0.4, III) BG-0.8, IV) BG-MP, V) BGII-0.4, VI) BGII-0.8; a) in the form of powders, b) embedded in the BC matrix (the pictures are representative for five analyses/specimens).

To determine obtained microstructure and formed porosities, the BC specimens were analyzed by SEM, both after production and after 30 days of exposure to PBS solution (Fig. 2). The addition of the BGs did not cause significant changes in the BC/BC-AgNp microstructure and all specimens had a structure typical for acrylic types of cement, with PMMA chains and free spaces. However, increased porosity of the BC matrix was particularly visible for BGII-0.8 and BGII-0.4, then BG-0.4 and BG-MP, with the weakest effect for BG-0.8.

Fig. 2. Microscope images of BC surfaces a,b – SEM, c,d – OM: after 30 days of PBS exposure: I) BC-AgNp, II) BC-BG-0.4-AgNp, III) BC-BG-0.8-AgNp, IV) BC-BG-MP-AgNp, V) BC-BGII-0.4-AgNp, VI) BC-BGII-0.8-AgNp; a) 100x magnification, b) 250x magnification, c) 200x magnification, d) cross-section 200x magnification (the pictures are representative for five specimens).

Furthermore, the distribution of BGs particles on the surface and cross-section of each BCs was analyzed with OM (Fig. 2 (c) and (d)) using a dark-field. However, some cement components such as barium sulfate, or benzoyl peroxide, were also revealed in the specimens, such as BC-AgNp (Fig. 2: Ic) and Id)). The particles were located randomly in the BC matrix, but the distribution was relatively even. The exception was the incorporation with BG-MP, where clusters were formed as a result of particles` agglomeration.

3.2 Setting properties

The addition of particles did not significantly affect the setting properties of BC, except BG/BGII-0.8 (Table 2). All modified BCs had curing time in the range of 14–18 min and the maximum polymerization temperature in the range of 34–42 °C.

Table 2. Setting properties of the tested bone cements (n=3; data are expressed as the mean ± SD)

	Curing time [min]	Maximum polymerization temperature [°C]
BC	15:30 ± 0:40	37.6 ± 1.2
BC-AgNp	15:50 ± 1:10	40.5 ± 1.4
BC-BG-0.4-AgNp	16:10 ± 0:50	37.4 ± 1.1
BC-BG-0.8-AgNp	16:30 ± 1:10	36.3 ± 1.6*
BC-BGII-0.4-AgNp	15:40 ± 1:30	38.2 ± 0.8
BC-BGII-0.8-AgNp	16:40 ± 1:20	35.6 ± 1.4*
BC-BG-MP-AgNp	16:20 ± 2:10	36.8 ± 2.4

* statistically significant difference as compared to the BC-AgNp ($p < 0.05$), # statistically significant difference as compared to the BC ($p < 0.05$)

3.3 Chemical analysis

The chemical composition of tested BCs was studied by the FTIR method and is shown in Fig. 3 and Table 3. The spectrum of neat BC shows peaks at ~2950 cm^{-1} for methylene (CH2) and the methyl (CH3) stretches, at ~1720 cm^{-1} for the C=O stretch, at 1400 and 1450 cm^{-1} for groups CH2 and CH3, at 1240 cm^{-1} for the C–C–O stretch, at 1140 cm^{-1} for the O–C–C stretch and 950 cm^{-1} for C–O stretch[56]. The incorporation with BGs and AgNP did not change the chemical composition of the BC matrix as there was no formation of new chemical groups. The similar spectra, in the same peaks position and magnitude of intensity, were observed in all modified BCs compared to the control – unmodified material. Moreover, typical peaks from BGs were not found in the tested spectrum, i.e. Si-O-Si (~1050 cm^{-1}), Si-O (~830 cm^{-1}), B-O (~1000/1350 cm^{-1}) and P-O (~580 cm^{-1}) stretches[57], which might be caused by the overlapping by the peeks belonged to neat BC.

Table 3. FTIR wavenumbers for selected characteristic peaks of tested bone cements (the results are representative for five specimens).

	FTIR wavenumber of characteristic peaks [cm^{-1}]				
	CH2,CH3	C=O	C–C–O	O–C–C	C–O
BC	2938	1719	1240	1139	950
BC-AgNp	2950	1719	1232	1136	953
BC-BG-0.4-AgNp	2948	1721	1236	1139	951
BC-BG-0.8-AgNp	2948	1722	1240	1138	950
BC-BGII-0.4-AgNp	2953	1719	1240	1140	952
BC-BGII-0.8-AgNp	2951	1722	1239	1137	950
BC-BG-MP-AgNp	2947	1724	1241	1140	950

Fig. 3. FTIR spectra of tested bone cements (the pictures are representative for five specimens).

3.4 Wettability

View Article Online
DOI: 10.1039/D1BM00070A

The wettability results are shown in Fig. 4. The incorporation of the BGs significantly increased the values of BC/BC-AgNp contact angles to around 80°.

Fig. 4. Surface wettability of the tested bone cements determined by the measurements of the contact angle of distilled water (n=5; data are expressed as mean ± SD; * statistically significant difference as compared to the BC/BC-AgNp ($p < 0.05$)).

3.5 Mechanical properties

The mechanical properties of BCs, as hardness and reduced Young's Modulus, before and after 30-days PBS exposure, are shown in Table 4. The incorporation of BGs to BC-AgNp did not significantly affect its hardness but considerably influenced Young's modulus. The BGs with a smaller particle size: BG-0.4 and BGII-0.4 increased Er approximately by 20%. However, Er of other BGs, such as BG-0.8, BGII-0.8, and BG-MP, decreased approx. by 10-18%.

Table 4. Mechanical properties for tested bone cements (n=10; data are expressed as the mean ± SD)

	Hardness (GPa)		Reduced Young's modulus (GPa)	
	Before PBS exposure	After PBS exposure	Before PBS exposure	After PBS exposure
BC-AgNp	0.189 ± 0.020	0.182 ± 0.023	3.893 ± 0.461	3.599 ± 0.179
BC-BG-0.4-AgNp	0.196 ± 0.018	0.193 ± 0.017	4.742 ± 0.221*	4.819 ± 0.239*
BC-BG-0.8-AgNp	0.167 ± 0.023	0.161 ± 0.018*	3.482 ± 0.307*	3.759 ± 0.270*
BC-BGII-0.4-AgNp	0.195 ± 0.024	0.169 ± 0.015#	4.704 ± 0.227*	4.171 ± 0.163*#
BC-BGII-0.8-AgNp	0.179 ± 0.019	0.164 ± 0.019	3.128 ± 0.126*	2.332 ± 0.106*#
BC-BG-MP-AgNp	0.173 ± 0.044	0.169 ± 0.011	3.185 ± 0.347*	3.122 ± 0.157

* statistically significant difference as compared to the BC-AgNp ($p < 0.05$), # statistically significant difference as compared to the BC ($p < 0.05$)

Exposure to the PBS solution had no significant effect on the hardness of the specimens, except for a slight decrease of BC-BGII-04-AgNp. A significant decrease of Er was observed after exposure for the BC with the incorporation of BGII-0.4 (~11%) and BGII-0.8 (~25%).

3.6 PBS exposure and UV-Vis analysis

Exposure of the tested BC specimens to the PBS solution for 30 days did not significantly affect their structure, but a slight improvement in porosity was observed (Fig. 2). Moreover, the weight loss of all specimens appeared (Fig. 5). The smallest loss of weight was found from the reference materials BC (~0.3%) and BC-AgNp (~0.4%), while the weight of all BCs incorporated with BGs exceeded 1%. The weight of BCs with BG-MP and BG-0.8 decreased by ~1-2%, the BG-0.4, BGII-0.4 and BGII-0.8 by 2-2.5%.

Fig. 5. Weight loss of tested bone cement after monthly exposure to PBS solution (n=3; data are expressed as mean ± SD; * statistically significant difference as compared to BC/BC-AgNp ($p < 0.05$))

The UV-Vis spectra of PBS solutions with BC specimens after 1, 7, and 30 days are shown in Fig. 6. A strong absorption band at 200-250 nm was observed in all solutions, which could be attributed to PMMA (200 nm) and MMA (250 nm)[46]. Compared to control – BC-AgNp, the incorporation of BGs, especially BG-II-0.8, BG-0.4 and BG-II-0.4, increased the release of MMA.

Fig. 6. UV-VIS spectra of the PBS solutions immersed bone cements after 1 day (a), 7 days (b) and 30 days (c) (the spectra are representative for three specimens)

Furthermore, the incorporation of BGs affected the release of AgNp from the BC matrix (Fig. 6). According to the reference, AgNp water solution (S.Fig.1), the highest absorption band of the AgNp was observed at 270 nm (S.Fig.1). As seen in the insets of Fig. 6, the same signal was detected in the spectra of all specimens. Analysis of the results revealed that in BGII-0.4, BGII-0.8, and BG-0.4 the release of AgNp begun earlier than in other samples (after 1 day of incubation). Also, for these specimens, the release of AgNp was the highest. Compared to the control (BC-AgNp), it indicated that the addition of all BGs except BG-0.8 would be beneficial for accelerating the AgNp release.

3.7 Hemocompatibility

Table 5 showed the hemolysis rate and the LDH release in the supernatant after 24 exposure of RBCs to the BCs. For all tested specimens, the hemolysis rate and LHD in supernatant did not exceed 5% and LDH in supernatant 15.0 µmol/min/1012 RBC, respectively[58]. Compared to the control samples and control specimens (BC/BC-AgNp), it indicated that the incorporation of BGs did not induce any severe hemolytic reaction.

Table 5. The hemolysis rate and the LDH release after *in vitro* 24 h exposure of RBCs to tested bone cement specimens (n = 3; data are the means ± SD)

	Hemolysis		LDH in supernatant	
	absorbance	(%)	µmol/min/10^{12} RBC	(%)
BC	0.048 ± 0.029	0	4.94 ± 3.25	3.09
BC-AgNp	0.056 ± 0.019	0.2	7.28 ± 4.96	5.11
BC-BG-0.4-AgNp	0.137 ± 0.139*#	2.9	8.65 ± 3.60	6.28
BC-BG-0.8-AgNp	0.059 ± 0.014	0.3	4.49 ± 9.90	2.71
BC-BGII-0.4-AgNp	0.061 ± 0.013	0.4	3.52 ± 1.48	1.88
BC-BGII-0.8-AgNp	0.086 ± 0.046	1.2	5.47 ± 3.30	3.55
BC-BG-MP-AgNp	0.051 ± 0.017	0.1	4.93 ± 2.88	3.09
Control positive	>3.0	> 60 times – 100%	116.54 ± 49.92	100
Control negative	0.050 ± 0.033	0	1.33 ± 1.42	0

* statistically significant difference as compared to negative control ($p < 0.05$)

Furthermore, the platelet viability and aggregation after the 2h exposure of PLTs to tested BCs are shown in Table 6. Exposure of PLTs to the BCs did not induce spontaneous PLTs aggregation and there were no significant changes in thrombin-induced aggregation. However, such an exposure slightly reduced the late phase of aggregation. A significant reduction in PLTs viability was found only for the BC with BGII.

Table 6. Platelet aggregation and MTT after *in vitro* 2h exposure to tested bone cement specimens (n = 3; data are the means ± SD)

	Platelet aggregation (%)		Platelet viability (% of control)
	1 min after Thrombin-evocation	10 min after Thrombin-evocation	
BC	31.3 ± 9.6	65.7 ± 10.6	107.1 ± 1.0
BC-AgNp	21.3 ± 14.2	54.0 ± 26.2	76.1 ± 18.5
BC-BG-0.4-AgNp	21.3 ± 15.0	61.3 ± 11.0	105.7 ± 60.1
BC-BG-0.8-AgNp	16.0 ± 13.1	43.3 ± 28.0	113.9 ± 76.3
BC-BGII-0.4-AgNp	2.3 ± 1.2*	36.0 ± 10.5	62.9 ± 8.1*
BC-BGII-0.8-AgNp	23.0 ± 15.9	53.3 ± 26.7	63.7 ± 8.9*
BC-BG-MP-AgNp	21.0 ± 11.8	55.3 ± 9.1	125.4 ± 82.5
Control positive	2.7 ± 2.5	3.0 ± 1.0	9.8 ± 3.6
Control negative	26.3 ± 15.6	66.0 ± 10.5	100 ± 5.5

* statistically significant difference as compared to negative control ($p < 0.05$)

3.8 Cytocompatibility

The viability of PDLCs after 7 days of culture on tested BCs is presented in Fig. 7. The viability of PDLCs cultured on the tested BCs

significantly decreased compared to that on neat BC. The incorporation of different BGs to BC-AgNp had decreased cell viability. Whereas, BG decreased PDLC viability approx. by 30% compared to BC, the addition of BGII and BG-MP decreased cell viability drastically (approx. by 95%). Interestingly, the viability of PDLC was slightly higher on BC-BG-AgNp compared to BC-AgNp. It can be assumed that the addition of BG to BC-AgNp does not affect PDLC growth, in contrast to BGII and BG-MP addition that resulted in high cell cytotoxicity.

Fig. 7. PDLC viability on tested bone cements after 7-day culture. Results are expressed as a percentage in cell viability compared to the cell viability on the neat bone cement (n = 3; data are expressed as the mean ± SD; * statistically significant difference as compared to BC-AgNp ($p < 0.05$); # statistically significant difference as compared to BC ($p < 0.05$))

Besides, the morphology of PDLCs in the close proximity to the tested BCs was compared to cell morphology grown on TCP. This is shown in SFig. 2 and the results are consistent with those for the MTS viability tests. Neat BC, BC-AgNp, and BC-BG-0.4-AgNp did not affect the PDLCs morphology, and the confluent monolayer could be observed. For BC-BG-0.8-AgNp and BC-BGII-0.8-AgNp fewer cells were observed, but most cells were still spread and displayed typical fibroblastic morphology. In contrast, the toxicity of BC-BGII-0.4-AgNp and BC-BG-MP-AgNp was evident as most cells were rounded, not adhering well to the plates, likely to cell necrosis.

3.9 Antibacterial properties

The growth inhibition of selected bacteria incubated with BC specimens in the liquid environment is shown in Table 7. The addition of antibacterial agents, antibiotic and AgNp, to BCs significantly slowed down their growth comparing with the observed rapid multiplication for neat BC. Comparing the hospital strain with the reference strain of *S. aureus*, it can be seen that both modifiers are less effective against the hospital one. For reference bacteria, the growth inhibition of BC-A was stronger than that of BC-AgNp, whereas, for the hospital strain of *S. aureus*, BC-AgNp exhibited greater effectiveness. Incorporation of BG to BC-AgNp significantly improved its antibacterial effectiveness, especially in the case of BGII-0.04. This additive increased the growth inhibition of *S. aureus* ~20% (data after 3h) and *E. coli* about ~10% (data after 1h) compared to BC-AgNp or ~30-35% of *S. aureus* and ~15% of *E. coli* compared to neat BC.

Table 7. Bacterial growth inhibition determined by McFarland standard values specifying the number of selected bacteria during incubation with the tested BC specimens (n = 3; the max. SD is 0.03)

		BC	BC-AgNp	BC-BG-0.4-AgNp	BC-BG-0.8-AgNp	BC-BGII-0.4-AgNp	BC-BGII-0.8-AgNp	BC-BG-MP-AgNp	BC-A
S. aureus ATCC 29213	0h	0.5							
	0.5h	1.05#	0.95*	0.85*,^	0.93*,#,^	0.94*,^	1.01*	0.74*,^	1.02#
	1h	1.66#,^	1.06*,#,^	1.33*,#,^	1.43*,#,^	1.12*	1.21*,#	1.14*,#	1.17*,#
	2h	2.39#,^	1.50*,^	1.39*,#,^	2.11*,#,^	1.36*,#	1.85*,#,^	1.76*,#,^	1.3*,#
	3h	2.85#,^	2.36*,^	2.11*,#,^	2.33*,^	1.88*,#,^	2.00*,#,^	2.15*,#	2.22*,#
	4h	>4	>4	>4	>4	3.74	>4	>4	>4
S. aureus hospital strain	0h	0.5							
	0.5h	0.99	1.02	0.98	0.98	0.90*,#,^	1.12*,#,^	0.98	0.98
	1h	1.21	1.25^	1.22	1.25*	1.06*,#,^	1.20	1.04*,#,^	1.15#
	2h	2.10#,^	1.85*	1.75*,#	1.95*,#,^	1.60*,#,^	2.05#,^	1.95*,#,^	1.80*
	3h	2.97#,^	2.70*,^	2.58*,#,^	2.88*,#,^	2.11*,#,^	2.42*,#,^	2.16*,#,^	3.06*,#
	4h	>4	>4	>4	>4	3.62*,#,^	>4	>4	>4
E. coli ATCC 25922	0h	0.5							
	0.5h	1.65	1.62	1.62	1.73	1.61*,#,^	1.64	1.60	1.58
	1h	2.52#,^	2.32*,^	2.25*,#	2.30*	2.12*,#,^	2.25*,#	2.42*,#,^	2.23*,#
	2h	>4							

* statistically significant difference as compared to BC ($p < 0.05$); # statistically significant difference as compared to BC-AgNp ($p < 0.05$); ^ statistically significant difference as compared to BC-A

View Article Online
DOI: 10.1039/D1BM00079A

Furthermore, the bactericidal effectiveness against *S. aureus* hospital strain of the BC-BG-0.4-AgNp and BC-BGII-0.4-AgNp was evaluated (Fig. 8). Neat BC and BC-A (gentamicin-loaded) were selected as controls. The experiment confirmed the bactericidal properties of AgNp and the ability of antibacterial protection for modified BCs in test conditions. After exposure to neat BC, the bacteria multiplied in the agar plates ($3x10^8$ CFU/ml), whereas during the exposure to modified BC: BC-A, BC-BG-0.4-AgNp and BC-BGII-0.4-AgNp, the number of bacteria was significantly reduced ($2x10^4$, $5x10^4$, 0 CFU/ml, respectively). The best result of almost 100% killing of bacteria was observed for BC-BGII-0.4-AgNp. These results are consistent with the previous experiments.

Fig. 8. Comparison of bactericidal effectiveness against hospital strain of *Staphylococcus aureus* after its exposure to the tested BC (the pictures are representative for three experiments)

4 Discussion

Despite the natural self-healing ability, bone treatment is still a challenge in clinical routine. Some bone defects cannot be spontaneously repaired and biomaterials may be a promising tool to support their regeneration[59]. The following synthetic groups of bone substitutes have been currently developed, including bioceramics (calcium sulfate, calcium phosphate, bioactive glass), biometals (Ti-, Mg- and Fe-based alloy), and biopolymers (polymethyl methacrylate, polylactic acid, and polycaprolactone)[60,61]. Compared to those specified groups of biomaterials, acrylic bone cement still exhibits particularly favorable properties, like sufficient mechanical resistance, easy processability, injectable capability, and also relatively inexpensive cost[62]. Moreover, the proposed by us, AgNp-loaded BC is a valuable alternative to the currently used cements doped with antibiotic/s, but it still has some drawbacks. Therefore, the BGs have been introduced into BCs to obtain time-varying porosity and increase AgNp release rate. Our results show that the incorporation of BG into BC has different effects on cement physical, mechanical and biological properties, depending on BG type and particles size.

Effect of bioactive glasses on polymerization process

None of the tested BGs did significantly affect the polymerization process and all modified BC possessed a structure typical for PMMA cements (Fig. 2)[63,64]. Given that FTIR analysis did not shown significant changes in absorption spectra of analyzed specimens, we could assume that no chemical bonds between BGs and MMA were formed in the BC matrix. Furthermore, the SEM examinations showed the BGs particles were embedded in the structure (Fig. 1.). These results are in line with our previous and studies of others which have demonstrated the depositing different particles in BCs pores or voids between the chains[26,63,64]. The incorporation of BGs did not affect the setting parameters of BCs (Table 2). All modified BCs may be suitable for clinical application, as their curing time is in the range of 14-18 min and polymerization temperature in the range

of 34-39°C[65,66]. As shown in our earlier report[67], the addition of AgNp into BC increases the polymerization temperature by ~5-10%. On the contrary, the addition of BGs decreases this temperature, in particular for larger BGs particles, namely by ~10-12% for BC-AgNp and ~3-4% for BC. It seems a highly beneficial issue for the clinical application, as high polymerization temperature may cause protein denaturation, trigger apoptosis, or enhance inflammation[68]. The effects of different modifiers on setting parameters of BCs were already reported[26,69,70]. In particular, Samad et. al. observed that increasing the content of BGs filler (4-16 wt.%) in the PMMA-based cement composite decreased the polymerization temperature and enhanced curing time[39], which is in good agreement with the presented results.

Effect of bioactive glasses on wettability

The addition of BGs influenced the wettability of BCs as the contact angle increased to ~80° (Fig. 4), It is well-known that the surface of the biomaterial should be hydrophilic to ensure cell adhesion so that the contact angle is not to be over 90°. The change of BC wettability, after similar modification, was observed previously[26,71,72]. Untreated BGs are generally characterized by slightly hydrophobic properties, e.g. the BGs scaffolds show a contact angle ~110° [73] and BGs coating about ~95-105° [74]. However, neat BCs or BC-AgNps display much lower contact angles, 50-60°. Despite the decrease of modified BCs wettability resulting from different contact angles of both components, all tested BCs remain hydrophilic, and thus they are acceptable for a bone-substitute material.

Effect of bioactive glasses on porosity

The introduction of BGs affects the porosity as illustrated by SEM observations (Fig. 2) and the weight loss (Fig. 5). After PBS exposure, tested composites displayed greater porosity and the BGs behave as porogens. Puska et al. investigated a similar composite with BGs filler (30 wt.%), stating that the material had a porous structure after water sorption[40]. The most significant improvement in our studies was observed for BGII due to its high water solubility[75]. Achieving a partially biodegradable structure results in the gradual opening of new pores and channels, which contribute to the moderate release of active substances from the BCs.

Effect of bioactive glasses on bioactivity

In the current study, the bioactivity was assumed as the capability of the material to produce the apatite layer after exposure to PBS (Fig. 2). However, we did not observe such a phenomenon for any tested composite. Arcos et. al. previously reported the growth of the hydroxycarbonate layer on the surface of BG-PMMA composite, but the content of glass was as high as 55 wt.%[33]. We believe that the 5 wt.% of BG applied here is insufficient to initiate the apatite-like layer formation as only the BGs and not BC may attract the phosphate molecules.

Effect of bioactive glasses on MMA monomer release

The inclusion of BGs in the BCs and the increase of matrix porosity resulted in an increasing amount of unreacted MMA monomer (Fig. 6). The BGII and BG-0.4 increased MMA release to the greatest extent due to their highest water solubilities, and also increased porosity of the composite. The presence of unreacted monomer is a typical phenomenon for PMMA cements, and due to their low porosity, most of the monomer is permanently enclosed in the matrix[26,63]. The incorporation of biodegradable components, such as BGs, increases the BCs porosity, and simultaneously the release of MMA monomer by creating new pores and channels.

Effect of bioactive glasses on mechanical properties

The BGs addition into BC influenced mainly Young's modulus to depending on the size and distribution of BGs particles (Tab. 4). The neat BC tested by nanoindentation technique (Cemex, Tecres) had Er about 3.5-4.8 GPa and hardness about 0.14-0.2 GPa[24]. The tested BC-AgNp had similar mechanical parameters (Er ~3.4-4.5 GPa and H ~0.16-0.2 GPa). The obtained nanomechanical parameters of BC are consistent with the previously reported values, Er ~4-6 GPa and H ~0.15-0.30 GPa, depending on the type of BC and its production methods[49,76]. Generally, in the case of BC, it is suggested that the addition of different modifiers, depending on their size, shape, and type as well as their distribution, may have a various effect on mechanical properties[65,77,78]: (1) decreasing them as a result of weakening the polymerization reaction, increasing the distance between PMMA chains and improving internal porosity or (2) increasing them by filling the pores/free spaces in the matrix, affecting the distribution of PMMA chains and reducing internal porosity. In this study, we have found that the incorporation of BGs into BC had various impact mainly on Young's modulus depending mostly on the size and distribution of BGs particles. The increase of Er and H were observed for smaller particles (BGs-0.4) that may be related to the doping reinforcing effect. Such a phenomenon after BC modification was already suggested[15,65,79]. However, the decrease of Er and H found for large particles (BGs-0.8) and BG-MP was often observed for the composite or sandwich structures, also for doped BC, and may be caused by significant stress discontinuity or inhomogeneous structure instability[69,78,80]. The weakening of mechanical properties of modified BCs after monthly PBS exposure is a phenomenon due to matrix porosity appearing as a consequence of the dissolution of BGs particles[26]. Moreover, the BCs doped with BGs show better mechanical parameters than those doped with chitosan or tri-calcium phosphate which we have previously tested[26]. In similar work, Funk et. al. reported that BC containing BGs (~14 wt.%) could be suitable for weight-bearing applications[42]. However, for BC-BGII-0.8 and BC-BG-MP we have observed a significant decrease in mechanical properties after PBS exposure that requires future research.

Effect of bioactive glasses on hemocompatibility

Both, neat BC and some BGs are approved by the U.S. Food and Drug Administration for certain clinical applications[5,81]. After the introduction into the body, BCs may affect blood components and induce dangerous erythrocytes hemolysis or disturb hemostasis due to hyperactivation or even inactivation of blood platelets leading to thrombosis and bleedings. The present studies showed that

incorporation of all tested BGs had no negative short-term effect on the hemocompatibility of BC, as the hemolysis was not induced and the blood platelets still retained their control activity (Tab. 5 and 6). However, we found a significant reduction of PLTs viability exposed to BGII. Overall, modified BCs do not affect erythrocytes integrity, and blood platelet metabolism and activation, with an exception of BGII.

Effect of bioactive glasses on cytocompatibility

As the BC is a bioinert material that may release a toxic MMA monomer it has been important to verify its cytocompatibility after modification. Based on previous research[26], we assumed that the selection of small particles with osteoinductive features should improve the biocompatibility. However, the BGs incorporation into BC affected PDLC viability and morphology related to the type and size of BGs particles (Fig. 7 and SFig.2). The BG added into BC-AgNp slightly increased cells viability, while BGII and BG-MP decreased it significantly. Such effects may be attributed to the BGs addition. Generally, BGs are considered biocompatible, but the process of their degradation may cause a local increase in pH and negatively affect cell response. Also, BGIIs containing boron is considered toxic for cells when its concentration exceeds a certain level[82,83]. Moreover, the problem of cytotoxicity after BC modification may be related, at least in part, to the unreacted MMA monomer release (Figs. 5, 6 and S2). In support of the above, is the finding that BC-AgNp with BG-0.8 displayed the highest cell viability, whereas the amount of MMA released from these specimens after 7 days was the lowest. For, the BC with BGII-0.4/0.8, due to their significant solubility, the released amount of MMA was the highest, resulting in the cytotoxic effects of these composites. However, the results for BC-AgNp with BG-MP and BG-0.4 are not consistent with the assumption. For the BC with BG-MP, the release of MMA was quite low, but cytotoxic effect was still observed. Further, BC-BG-0.4-AgNp displayed the highest MMA release, but cell viability was improved as compared to BC-AgNp. These results suggest that the released amount of MMA is not only a single factor affecting the cytocompatibility of the modified BCs. The other reason can also be associated with in the bioactivity of studied BGs and different conversion rates to hydroxyapatite for the 45S5 and 1393B3 BGs accompanied by a local change of pH[84]. The potential BGs toxicity was also considered, particularly as being in the form of nanoparticles[85,86]. BGs content may also be an important factor influencing cellular response as previously reported[84,86]. Summarizing, the problem is complex and need further studies.

Effect of bioactive glasses on antibacterial efficiency

All tested BC-AgNp doped with BGs, except BG-0.8, demonstrated significant antibacterial efficiency (Fig. 6). The increased amount of released AgNp from partially degradable AgNp-loaded BC improved its antibacterial effectiveness. Enhanced antibacterial properties of BCs were already found for antibiotic-loaded BCs with the addition of BGs[42]. The determinants of the antibacterial efficiency were reported as the BG solubility and particle size (Tab. 7 and Fig. 8). BGs with a small size (BG-0.4) and greater solubility (BGII) contributed to a better release of AgNp resulting in more significant antibacterial effectiveness of BC. BG-MP does not exhibit the above trend, which may be related to its agglomeration and uneven distribution in the matrix (Fig. 1). Our studies also confirm that BC-AgNp is more effective than antibiotic-loaded BC to inhibit antibiotic resistance of bacteria, it has bactericidal properties and after BGII-0.4 incorporation, it may completely kill all the bacteria on the surface. However, compared to our previous study, where BC-AgNp antibacterial properties were evaluated by the McFarland bacterial growth with inhibition test[25], in this study the antimicrobial properties of studied specimens significantly decreased. This may be due to the change of the sterilization method. In our previous studies, specimens were autoclaved, whereas in this work we exposed materials to ethanol only because of the use of biodegradable components, BGs, and this exposure could remove most of AgNp from the BC external layer.

Medical applications of composite cements

Based on obtained results, we can propose two different medical applications: (1) as bone substitutes, we would apply the BC-BG-0.4-AgNP, and (2) as spacers or in cancer therapy, we would suggest the BC-BGII-0.4-AgNp. If osteointegration is desirable, as for bone substitute material, an important aspect is to ensure appropriate cellular responses. However, when the key aspect is focused on local infection therapy or the delivery of a therapeutic agent into the tissue environment, full osteointegration is not important and it can be even disadvantageous, as typically such BC is used as a short-term implant. We assume that cytotoxicity of some modified BCs may not be observed *in vivo* due to the dynamic nature of tissue environment, body fluid circulation as well as the body's ability to metabolize and transport some ions or particles. However, these effects are potentially undesired and further research is aimed to focus on decreasing undesirable biological effects by, e.g. functionalization of BC-BG-AgNp matrix with an additional substance to achieve an interfacial bond between the matrix and the additives as well as to bind the unreacted MMA monomer into the non-toxic complex by some additional compounds, such as silanes.

Conclusions

Nanosilver-loaded PMMA bone cement doped with different bioactive glasses has been successfully fabricated and displayed several improved features. The incorporation of BGs (5 wt.%) significantly and positively affects the polymerization process (polymerization temperature) and antibacterial effectiveness, however, it slightly decreases wettability and mechanical properties. Mechanical properties of composite BCs depend mostly on the size and distribution of BGs particles due to the stability of the homogeneous structure. The most critical factor influencing the biological properties is the porosity of specimens. An excess porosity may cause an increased release of unreacted MMA and result in high cytotoxicity. The addition of small melted BGs particles (~40 µm) changes the microstructure and improves the properties of BCs due

to even distribution, such as more effective porosity, lower deterioration of mechanical properties, and significant antibacterial effect. Depending on the medical application, we can recommend the AgNp-loaded BC with the 45S5 BGs for bone substitutes, or AgNp-loaded cement with 13-93B3 as a coating for spacers or in drug delivery in cancer therapy.

Author Contributions

Conceptualization, M.W.; methodology, M.W., S.C., B.K., M.N., A.P., A.M., A.M.O and M.M.; formal analysis, M.W., A.M., A.M.O, M.M. and A.Z., investigation, M.W., S.C., B.K., M.N., K.Ł., A.P. and A.M.; data curation, M.W.; writing - original draft preparation, M.W.; writing - review and editing, M.W., A.M., A.M.O., M.M., and A.Z., project administration, M.W.; supervision, A.M and A.Z. All authors have read and agreed to the published version of the manuscript.

Conflicts of interest

There are no conflicts to declare.

Funding

This research was supported in part by the Polish National Science Centre, grant no. 2016/21/B/NZ5/00217 (A.M.O.); the Medical University of Gdańsk fund (A.M.), ST-57; the Polish National Agency for Academic Exchange (M.W.), dissemination activities of FunGlass project (M.M.); the European Union's Horizon 2020, grant. No. 739566.

Acknowledgements

The authors thank all those who contributed to preparing this paper, i.e., the team from the Biomaterials Group at the Gdańsk University of Technology (especially M. Bartmański and G. Gajowiec), the team from the Institute of Zoology and Biomedical Research (especially G. Tylko and K. Truchan) and the team from the Keyence International Company (especially D. Chojowski) for their technical assistance in some of the tests. Moreover, our appreciation, in particular, goes to the Higmed Poland s.c. for providing bone cements for the research.

References

1 K. Holkar, A. Vaidya, P. Pethe, V. Kale and G. Ingavle, *Materialia*, 2020, **12**, 100736.
2 N. Abbasi, S. Hamlet, R. M. Love and N. T. Nguyen, *Journal of Science: Advanced Materials and Devices*, 2020, **5**, 1–9.
3 W. Wang and K. W. K. Yeung, *Bioactive Materials*, 2017, **2**, 224–247.
4 Z. He, Q. Zhai, M. Hu, C. Cao, J. Wang, H. Yang and B. Li, *Journal of Orthopaedic Translation*, 2015, **3**, 1–11.
5 R. Vaishya, M. Chauhan and A. Vaish, *Journal of Clinical Orthopaedics and Trauma*, 2013, **4**, 157–163.
6 U. Ali, K. J. B. A. Karim and N. A. Buang, *Polymer Reviews*, 2015, **55**, 678–705.
7 W. Zhang, G. Lei, Y. Liu, W. Wang, T. Song and J. Fan, *Microbial Pathogenesis*, 2017, **102**, 42–44. View Article Online DOI: 10.1039/D1BM00079A
8 E. Prochazka, T. Soukup, M. Hroch, L. Fuksa, E. Brcakova and J. Cermanova, *International Orthopaedics*, 2010, **34**, 137–142.
9 T. Thielen, S. Maas, A. Zuerbes, D. Waldmann, K. Anagnostakos and J. Kelm, *International Journal of Medical Sciences*, 2009, **31**, 930–936.
10 D. G. Meeker, K. B. Cooper, R. L. Renard, S. C. Mears, M. S. Smeltzer and C. L. Barnes, *Journal of Arthroplasty*, 2019, **34**, 1458–1461.
11 E. Carlsson, G. Mestres, K. Treerattrakoon, A. López, M. K. Ott, S. Larsson and C. Persson, *BioMed research international*, 2015, **594284**.
12 E. Paz, Y. Ballesteros, F. Forriol, N. J. Dunne and J. C. del Real, *Materials Science and Engineering C*, 2019, **104**, 109946.
13 S.M.Z. Khaled, R.J. Miron, D.W. Hamilton, P.A. Charpentier and A. S. Rizkalla, *Dental Materials*, 2009, **6**, 169–178.
14 C. Fukuda, K. Goto, M. Imamura, M. Neo and T. Nakamura, *Acta Biomaterialia*, 2011, **7**, 3595–3600.
15 X. Lin, J. Ge, D. Wei, C. Liu, L. Tan, H. Yang, K. Yang, H. Zhou, B. Li, Z. P. Luo and L. Yang, *Journal of Orthopaedic Translation*, 2019, **17**, 121–132.
16 K. Letchmanan, S. C. Shen, W. K. Ng, P. Kingshuk, Z. Shi, W. Wang and R. B. H. Tan, *Journal of the Mechanical Behavior of Biomedical Materials*, 2017, **72**, 163–170.
17 C. Wolf-Brandstetter, S. Roessler, S. Storch, U. Hempel, U. Gbureck, B. Nies, S. Bierbaum and D. Scharnweber, *Journal of Biomedical Materials Research - Part B Applied Biomaterials*, 2013, **101**, 599–609.
18 Z. Liu, Y. Tang, T. Kang, M. Rao, K. Li, Q. Wang, C. Quan, C. Zhang, Q. Jiang and H. Shen, *Colloids and Surfaces B: Biointerfaces*, 2015, **131**, 39–46.
19 G. Azuara, J. García-García, B. Ibarra, F. J. Parra-Ruiz, A. Asúnsolo, M. A. Ortega, B. Vázquez-Lasa, J. Buján, J. San Román and B. de la Torre, *Revista Española de Cirugía Ortopédica y Traumatología*, 2019, **63**, 95–103.
20 T. Russo, A. Gloria, R. De Santis, U. D'Amora, G. Balato, A. Vollaro, O. Oliviero, G. Improta, M. Triassi and L. Ambrosio, *Bioactive Materials*, 2017, **2**, 156–161.
21 L. Cao, X. Xie, B. Wang, M. D. Weir, T. W. Oates, H. H. K. Xu, N. Zhang and Y. Bai, *Journal of Dentistry*, 2018, **79**, 39–45.
22 J. Martínez-Moreno, C. Mura, V. Merino, A. Nácher, M. Climente and M. Merino-Sanjuán, *Journal of Arthroplasty*, 2015, **30**, 1243–1249.
23 G. Frutos, J. Y. Pastor, N. Martínez, M. R. Virto and S. Torrado, *Acta Biomaterialia*, 2010, **6**, 804–811.
24 M. Wekwejt, N. Moritz, B. Świeczko-Żurek and A. Pałubicka, *Polymer Testing*, 2018, **70**, 234–243.
25 M. Wekwejt, A. Michno, K. Truchan, A. Pałubicka, B. Świeczko-Żurek, A.M. Osyczka and A. Zieliński, *Nanomaterials*, 2019, **9**, 1114.
26 M. Wekwejt, M. Michalska-Sionkowska, M. Bartmański, M. Nadolska, K. Łukowicz, A. Pałubicka, A. M. Osyczka and A. Zieliński, *Materials Science and Engineering C*, 2020, **117**, 2020.
27 Y. H. Luo, L. W. Chang and P. Lin, *BioMed Research International*, 2015, **2015**.
28 S. N. Sawant, V. Selvaraj, V. Prabhawathi and M. Doble, *PLoS ONE*, 2013, **8**, 1–9.
29 J. R. Jones, *Acta Biomaterialia*, 2015, **23**, 53–82.
30 F. Baino, *Ceramics International*, 2018, **44**, 14953–14966.
31 A. Hoppe, N. S. Güldal and A. R. Boccaccini, *Biomaterials*, 2011, **32**, 2757–2774.
32 M. Fernández, J. A. Méndez, B. Vázquez, J. San Román, M. P. Ginebra, F. J. Gil, J. M. Manero and J. A. Planell, *Journal of Materials Science: Materials in Medicine*, 2002, **13**, 1251–1257.

33 D. Arcos, C. V. Ragel and M. Vallet-Regí, *Biomaterials*, 2001, **22**, 701–708.
34 L. Floroian, C. Samoila, M. Badea, D. Munteanu, C. Ristoscu, F. Sima, I. Negut, M. C. Chifiriuc and I. N. Mihailescu, *Journal of Materials Science: Materials in Medicine*, 2015, **26**, 1–14.
35 X. Li and I. Zhitomirsky, *Progress in Organic Coatings*, 2020, **148**, 105883.
36 R. Ravarian, H. Wei, A. Rawal, J. Hook, W. Chrzanowski and F. Dehghani, *Journal of Materials Chemistry B*, 2013, **1**, 1835–1845.
37 M. A. González Corchón, M. Salvado, B. J. De La Torre, F. Collía, J. A. De Pedro, B. Vázquez and J. S. Román, *Biomaterials*, 2006, **27**, 1778–1787.
38 D. Durgalakshmi and S. Balakumar, *Physical Chemistry Chemical Physics*, 2015, **17**, 1247–1256.
39 H. A. Samad, M. Jaafar, R. Othman, M. Kawashita and N. H. A. Razak, *Bio-Medical Materials and Engineering*, 2011, **21**, 247–258.
40 M. Puska, N. Moritz, A. J. Aho and P. K. Vallittu, *Journal of the Mechanical Behavior of Biomedical Materials*, 2016, **59**, 11–20.
41 W. F. Mousa, M. Kobayashi, S. Shinzato, M. Kamimura, M. Neo, S. Yoshihara and T. Nakamura, *Biomaterials*, 2000, **21**, 2137–2146.
42 G. A. Funk, J. C. Burkes, K. A. Cole, M. N. Rahaman and T. E. McIff, *Journal of Bone and Joint Infection*, 2018, **3**, 187–196.
43 www.tecres.it
44 K. Zheng, N. Taccardi, A. M. Beltrán, B. Sui, T. Zhou, V. R. R. Marthala, M. Hartmann and A. R. Boccaccini, *RSC Advances*, 2016, **6**, 95101–95111.
45 W. Depczynski, R. Kazala, K. Ludwinek and K. Jedynak, *Materials*, 2016, **9**, 1–12.
46 X. S. Chai, F. J. Schork and E. M. Oliver, *Journal of Applied Polymer Science*, 2006, **99**, 1471–1475.
47 A. Karimzadeh and M. R. Ayatollahi, *Polymer Testing*, 2012, **31**, 828–833.
48 W. C. Oliver and G. M. Pharr, *Journal of Materials Research*, 1992, **7**, 1564-1583.
49 H.A. Shirazi, S.A. Mirmohammadi, M. Shaali, A. Asnafi and M.R. Ayatollahi, *Polymer Testing*, 2017, 59, 328-335.
50 NACO, *Journal of Chemical Information and Modeling*, 2013, **53**, 1689–1699.
51 M. Bakkar, Y. Liu, D. Fang, C. Stegen, X. Su, M. Ramamoorthi, L. C. Lin, T. Kawasaki, N. Makhoul, H. Pham, Y. Sumita and S. D. Tran, *Methods in Molecular Biology*, 2017, **1553**, 191–207.
52 J. F. Stevens, W. Tsang and R. G. Newall, *Journal of Clinical Pathology*, 1983, **36**, 1371–1376.
53 M. Weber, H. Steinle, S. Golombek, L. Hann, C. Schlensak, H. P. Wendel and M. Avci-Adali, *Frontiers in Bioengineering and Biotechnology*, 2018, **6**, 99.
54 A. Di Vito, A. Giudice, E. Chiarella, N. Malara, F. Bennardo and L. Fortunato, *Cell Transplantation*, 2019, **28**, 129–139.
55 A. Z. S. Ramirez-arcos, *Current Microbiology*, 2015, 907–909.
56 W. N. Ayre, S. P. Denyer and S. L. Evans, *Journal of the Mechanical Behavior of Biomedical Materials*, 2014, **32**, 76–88.
57 X. Liu, M. N. Rahaman and D. E. Day, *Journal of Materials Science: Materials in Medicine*, 2013, **24**, 583–595.
58 H. Jeong, J. Hwang, H. Lee, P. T. Hammond, J. Choi and J. Hong, *Scientific Reports*, 2017, **7**, 1–13.
59 V. Martin and A. Bettencourt, *Materials Science and Engineering C,* 2018, **82**, 363-371.
60 T. Winkler, F.A. Sass, G.N. Duda and K. Schmidt-Bleek, *Bone & Joint Research*, 2018, **7**, 232-243.
61 G. Fernandez de Grado, L. Keller, Y. Idoux-Gillet, Q. Wagner, A.M. Musset, N. Benkirane-Jessel, F. Bornert and D. Offner, *Journal of Tissue Engineering*, 2018, **9**, 1-18.
62 A.D. Bagde, A.M. Kuthe, S. Quazi, V. Gupta, S. Jaiswal, S. Jyothila, N. Lande and S. Nagdeve, *Innovation and Research in BioMedical Engineering*, 2019, **40**, 133-144.
63 S. Soleymani Eil Bakhtiari, H. R. Bakhsheshi-Rad, S. Karbasi, M. Tavakoli, S. A. Hassanzadeh Tabrizi, A. F. Ismail, A. M. Seifalian, S. RamaKrishnaan and F. Berto, *Polymer International*, 2020.
64 M. H. Pelletier, A. C. B. Lau, P. J. Smitham, G. Nielsen and W. R. Walsh, *Acta Biomaterialia*, 2010, **6**, 886–891.
65 M. Khandaker, M. B. Vaughan, T. L. Morris, J. J. White and Z. Meng, *International Journal of Nanomedicine*, 2014, **9**, 2699–2712.
66 J. Han, G. Ma and J. Nie, *Materials Science and Engineering C*, 2011, **31**, 1278–1284.
67 M. Wekwejt, D. Etmańska, A. Halman, A. Pałubicka, B. Świeczko-Żurek and G. Gajowiec, *Journal of Biomedical Materials Research - Part B Applied Biomaterials*, 2020, **108**, 2733–2742.
68 C. Robo, G. Hulsart-Billström, M. Nilsson and C. Persson, *Acta Biomaterialia*, 2018, **72**, 362–370.
69 S. Bong, Y. Jick, T. Lim, S. A. Park, I. Hee, E. Jung, I. Ae and J. Shin, *Biomaterials*, 2004, **25**, 5715–5723.
70 S. Gao, Y. Lv, L. Yuan, H. Ren, T. Wu, B. Liu, Y. Zhang, R. Zhou, A. Li and F. Zhou, *Polymer Testing*, 2019, **76**, 513–521.
71 S. Alidadi, A. Oryan, A. Bigham-sadegh and A. Moshiri, *Carbohydrate Polymers*, 2017, **166**, 236–248.
72 H. Tan, S. Guo, S. Yang, X. Xu and T. Tang, *Acta Biomaterialia*, 2012, **8**, 2166–2174.
73 M. J. Woźniak, A. Chlanda, P. Oberbek, M. Heljak, K. Czarnecka, M. Janeta and Ł. John, *Micron*, 2019, **119**, 64–71.
74 U. R. Eckstein, R. Detsch, N. H. Khansur, M. Brehl, U. Deisinger, D. de Ligny, A. R. Boccaccini and K. G. Webber, *Ceramics International*, 2019, **45**, 14728–14732.
75 J. Ning, A. Yao, D. Wang, W. Huang, H. Fu, X. Liu, X. Jiang and X. Zhang, *Materials Letters*, 2007, **61**, 5223–5226.
76 H. A. Shirazi, S. A. Mirmohammadi, M. Shaali, A. Asnafi and M. R. Ayatollahi, *Polymer Testing*, 2017, **59**, 328–335.
77 T. Kawaguchi, L. V. J. Lassila, H. Baba, S. Tashiro, I. Hamanaka, Y. Takahashi and P. K. Vallittu, *Journal of the Mechanical Behavior of Biomedical Materials*, 2020, **102**, 103513.
78 M. Eliana, V. Zapata, H. Mina, V. Blanca, J. San and L. Rojo, *International Journal of Molecular Sciences,* 2019, 12, 2938.
79 B. Liu, M. Li, B. Yin, J. Zou and W. Zhang, *Plos One*, 2015, 1–20.
80 R. A. Latour, S. D. Trembley, Y. Tian, G. C. Lickfield and A. P. Wheeler, *Journal of Biomedical Materials Research*, 2000, **49**, 498–505.
81 N. C. Lindfors, J. T. Heikkilä, I. Koski, K. Mattila and A. J. Aho, *Journal of Biomedical Materials Research - Part B Applied Biomaterials*, 2009, **90 B**, 131–136.
82 X. Wei, T. Xi, Y. Zheng, C. Zhang and W. Huang, *Journal of Materials Science and Technology*, 2014, **30**, 979–983.
83 Q. Z. Chen and G. A. Thouas, *Acta Biomaterialia*, 2011, **7**, 3616–3626.
84 W. Huang, D. E. Day, K. Kittiratanapiboon and M. N. Rahaman, *Journal of Materials Science: Materials in Medicine*, 2006, **17**, 583–596.
85 A. S. Bakry, Y. Tamura, M. Otsuki, S. Kasugai, K. Ohya and J. Tagami, *Journal of Dentistry*, 2011, **39**, 599–603.
86 M. Rismanchian, N. Khodaeian, L. Bahramian, M. Fathi and H. Sadeghi-Aliabadi, *Iranian Journal of Pharmaceutical Research*, 2013, **12**, 437–443.

View Article Online
DOI: 10.1039/D1BM00079A

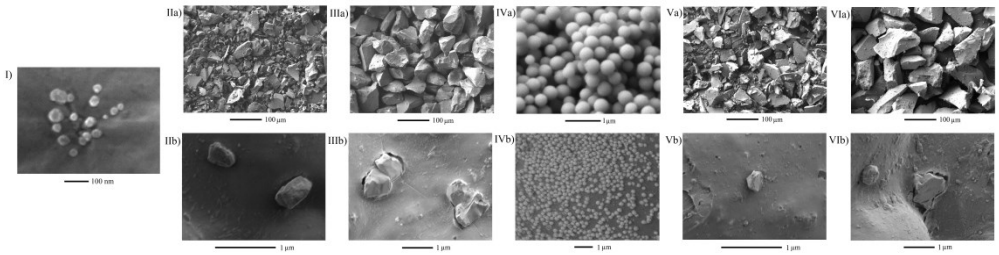

Fig. 1. SEM images of modifiers: I) AgNp, II) BG-0.4, III) BG-0.8, IV) BG-MP, V) BGII-0.4, VI) BGII-0.8; a) in the form of powders, b) embedded in the BC matrix

840x218mm (271 x 271 DPI)

View Article Online
DOI: 10.1039/D1BM00079A

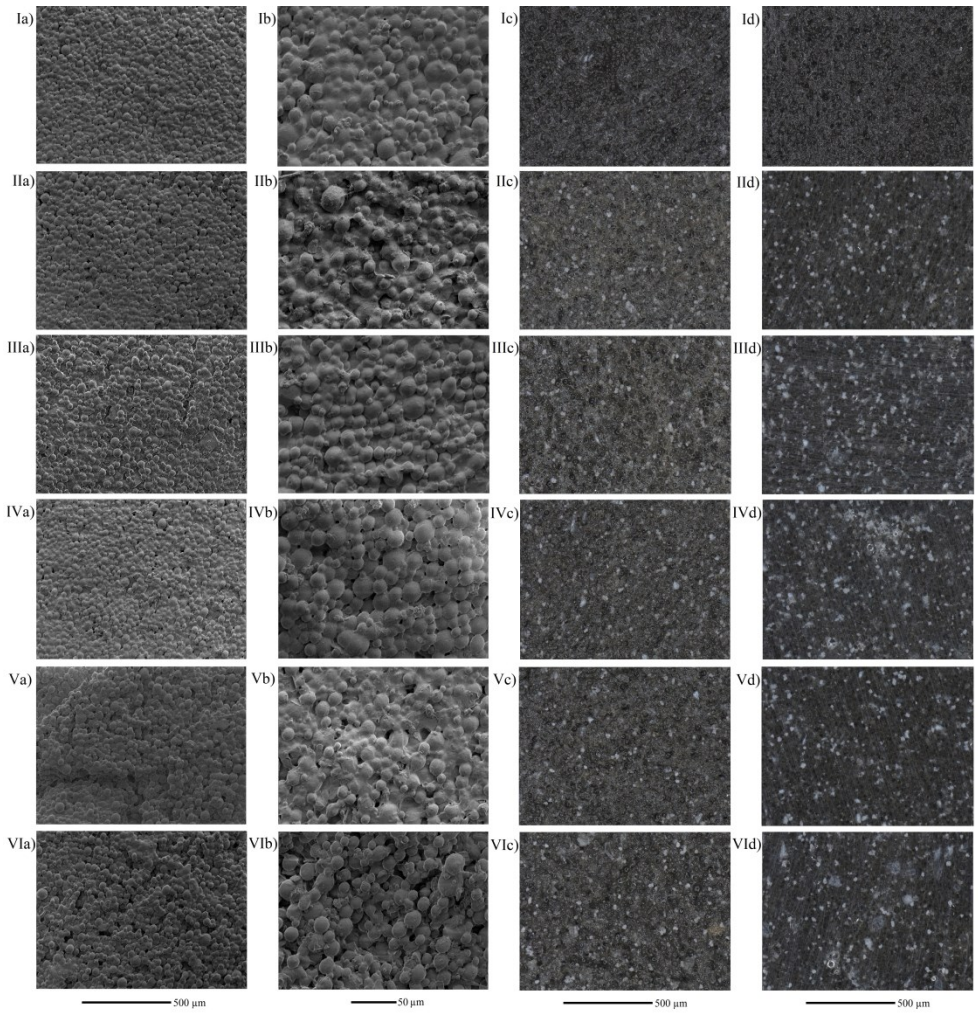

Fig. 2. Microscope images of BC surfaces a,b – SEM, c,d – OM: after 30 days of PBS exposure: I) BC-AgNp, II) BC-BG-0.4-AgNp, III) BC-BG-0.8-AgNp, IV) BC-BG-MP-AgNp, V) BC-BGII-0.4-AgNp, VI) BC-BGII-0.8-AgNp; a) 100x magnification, b) 250x magnification, c) 200x magnification, d) cross-section 200x magnification

571x575mm (271 x 271 DPI)

View Article Online
DOI: 10.1039/D1BM00079A

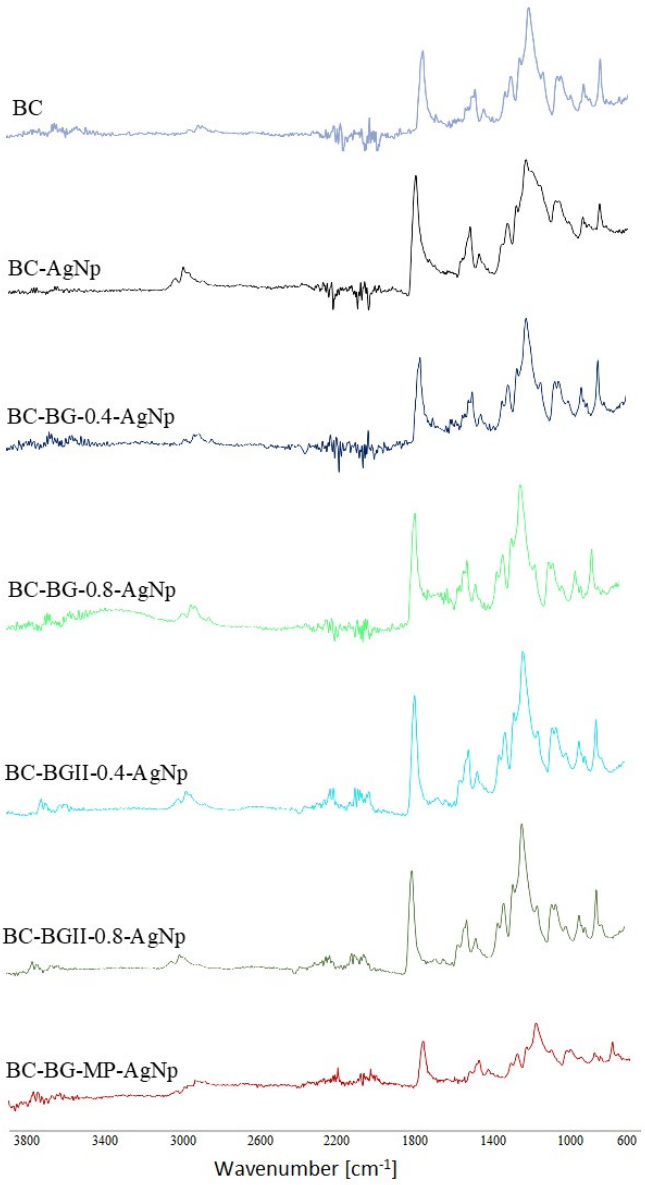

Fig. 3. FTIR spectra of tested bone cements

160x291mm (96 x 96 DPI)

View Article Online
DOI: 10.1039/D1BM00079A

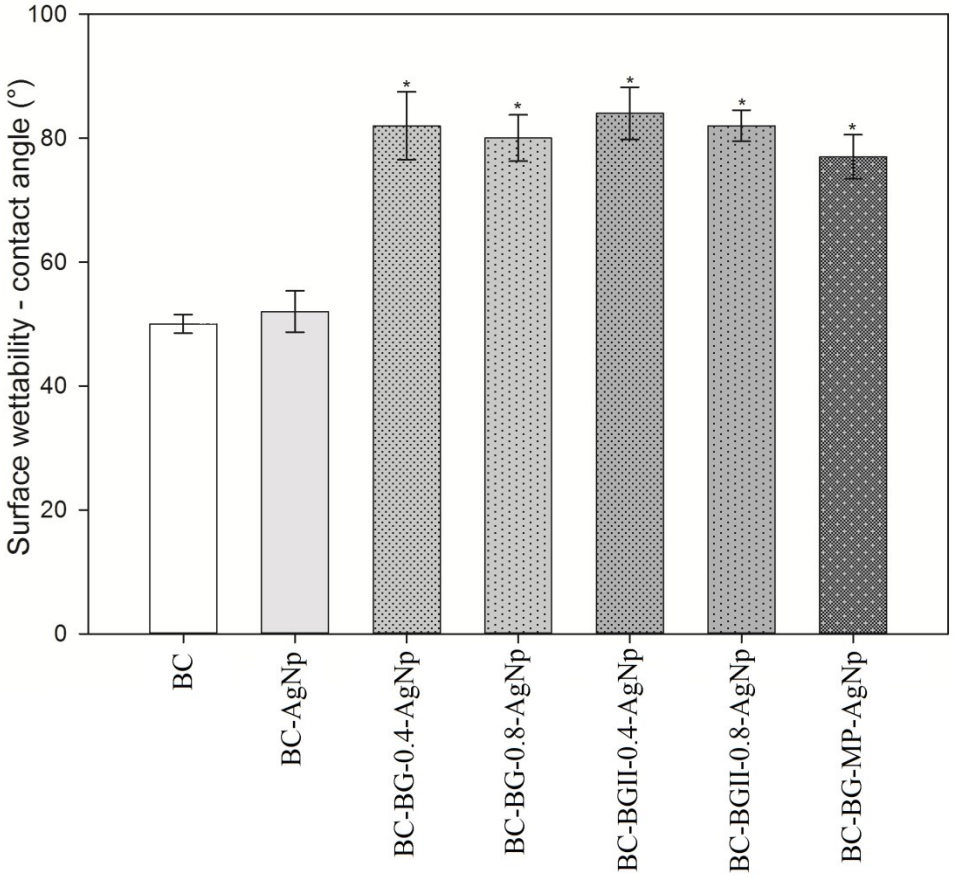

Fig. 4. Surface wettability of the tested bone cements determined by the measurements of the contact angle of distilled water

600x545mm (96 x 96 DPI)

View Article Online
DOI: 10.1039/D1BM00079A

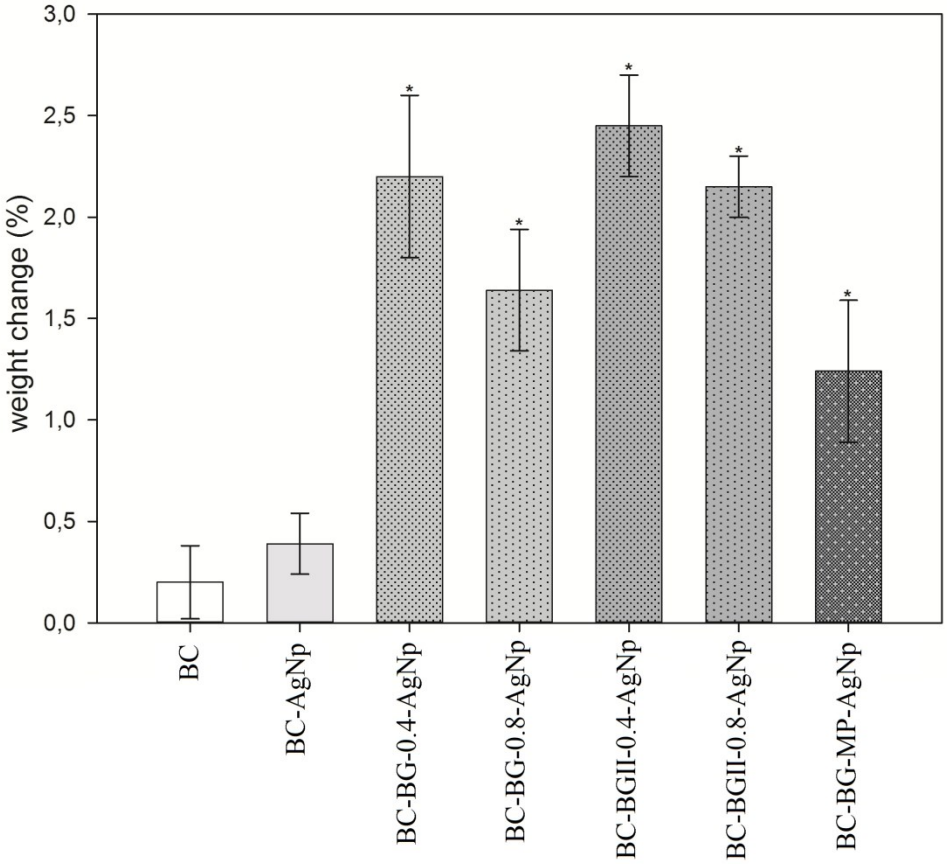

Fig. 5. Weight loss of tested bone cement after monthly exposure to PBS solution

610x548mm (96 x 96 DPI)

View Article Online
DOI: 10.1039/D1BM00079A

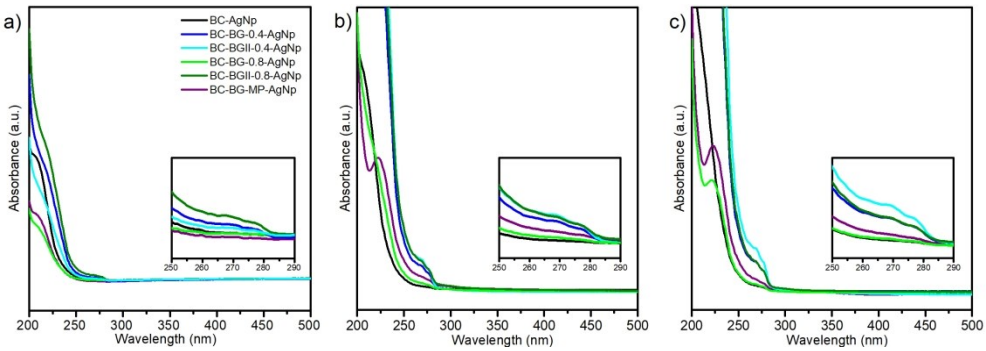

Fig. 6. UV-VIS spectra of the PBS solutions immersed bone cements after 1 day (a), 7 days (b) and 30 days (c)

211x72mm (300 x 300 DPI)

View Article Online
DOI: 10.1039/D1BM00079A

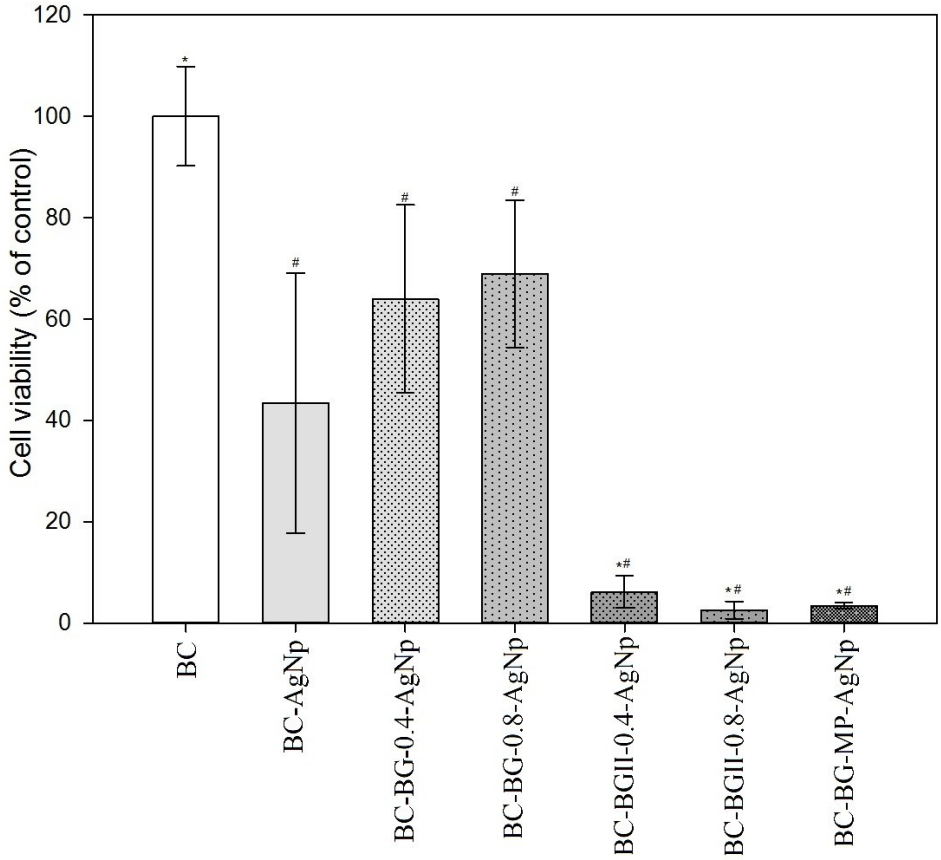

Fig. 7. PDLC viability on tested bone cements after 7-day culture. Results are expressed as a percentage in cell viability compared to the cell viability on the neat bone cement

195x179mm (150 x 150 DPI)

View Article Online
DOI: 10.1039/D1BM00079A

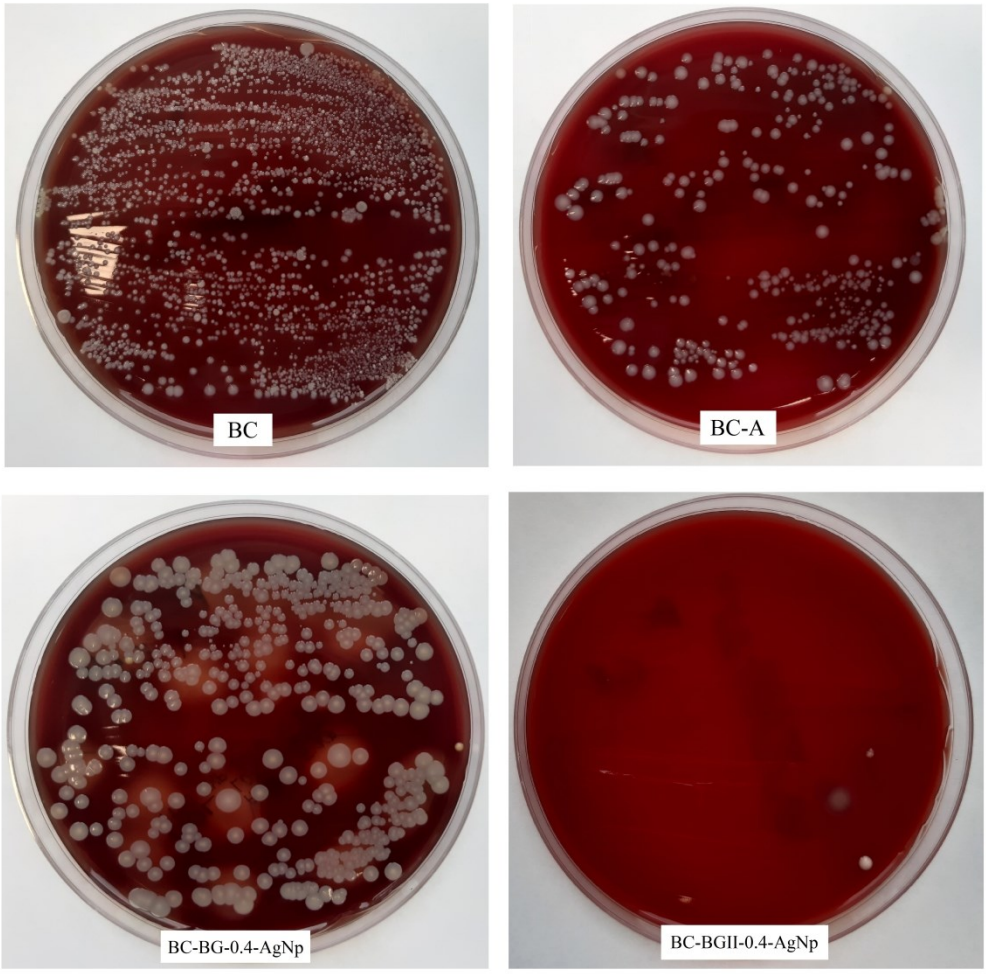

Fig. 8. Comparison of bactericidal effectiveness against hospital strain of Staphylococcus aureus after its exposure to the tested BC

1381x1382mm (96 x 96 DPI)